

# Deep subsurface imaging in tissues using spectral and polarization filtering

S. G. Demos, H. B. Radousky, and R. R. Alfano\*

Lawrence Livermore National Laboratory PO Box 808, Livermore, CA 94550

Demos1@lbl.gov

\* Institute for Ultrafast Spectroscopy and Laser, City College of New York, New York, NY, 10031

**Abstract:** Deep subsurface imaging in tissues is demonstrated by employing both spectral and polarization discrimination of the backscattered photons. This technique provides enhancement in the visibility of subsurface structures via processing of the depolarized images obtained using polarized illumination at different wavelengths. The experimental results demonstrate detection and imaging of a high-scattering object located up to 1.5-cm beneath the surface of a host chicken tissue used as the model medium.

©2000 Optical Society of America

OCIS codes: 290.1350 Backscattering, 170.3660 Light propagation in tissues, 170.3880 Medical and biological imaging

## References and Links

1. D. Huang, E. A. Swanson, C. P. Jin, J. S. Schuman, W. G. Stinson, W. Chang, M. R. Hee, T. Flotte, K. Gregory, C. C. A. Puliafito, and J. Fujimoto, Optical coherence tomography, *Science* **254**, 1178-1181 (1991).
2. W. Denk, J. H. Strickler, and W. W. Webb, 2-photon laser scanning fluorescence microscopy, *Science*, **248**, 73-76, (1990).
3. Y. C. Guo, P. P. Ho, H. Savage, D. Harris, P. Sacks, S. Schantz, P. Liu, N. Zhadin, R. R. Alfano, Second-harmonic tomography of tissues, *Opt. Lett.*, **22**, 1323 (1997).
4. Barry R. Masters, Andres Kriete, and Joig Kukulies, Ultraviolet confocal fluorescence microscopy of the invitro cornea - redox metabolic imaging, *Appl. Opt.*, **32**, 592-596 (1993).
5. S. G. Demos, R.R. Alfano, Temporal gating in highly scattering media by the degree of optical polarization, *Optics Lett.*, **21**, 161 (1996).
6. O. Emile, F. Bretenaker, A. LeFloch, Rotating polarization imaging in turbid media, *Opt. Lett.*, **21**, 1706 (1996).
7. G. Jarry, E. Steimer, V. Damaschini, M. Epifanio, M. Jurczak, R. Kaiser, Coherence and polarization of light propagating through scattering media and biological tissues, *Appl. Opt.*, **37**, 7357 (1998).
8. P. Gleyzes, A.C. Boccard, H. Saint-Jahnes, Multichannel Nomarski microscope with polarization modulation: performance and applications, *Opt. Lett.*, **22**, 1529 (1997).
9. S. G. Demos, W. B. Wang and R.R. Alfano, *Appl. Opt.*, **37**, Imaging objects hidden in scattering media with fluorescence polarization preservation of contrast agents, 792-797 (1998).
10. S.P. Schilders, X.S. Gan, M. Gu, *Appl. Opt.*, Resolution improvement in microscopic imaging through turbid media based on differential polarization gating, **37**, 4300 (1998).
11. J.S. Tyo, Enhancement of the point-spread function for imaging in scattering media by use of polarization-difference imaging, *J. Opt. Soc. Am. A*, **17**, 1 (2000).
12. S.K. Gayen, M.E. Zavallos, M. Alrubaiee, J.M. Evans, R.R. Alfano, Two-dimensional near-infrared transillumination imaging of biomedical media with a chromium-doped forsterite laser, *Appl. Opt.*, **37**, 5327 (1998).
13. S. G. Demos, H. Savage, Alexandra S. Heerdt, S. Schantz and R.R. Alfano, Polarization filter for biomedical tissue optical imaging, *Photochem Photobiol.*, **66**, 821 (1997).
14. A. H. Hilscher, J. R. Mourant, I. J. Bigio, Influence of particle size and concentration on the diffuse backscattering of polarized light from tissue phantoms and biological cell suspensions, *Appl. Opt.*, **36**, 125 (1997).
15. B.D. Cameron, M.J. Rakovic, M. Melnubeeglu, G.W. Kattawar, S. Rastegar, L.V. Wang, G.L. Cote, Measurement and calculation of the two-dimensional backscattering Mueller matrix of a turbid medium, *Opt. Lett.*, **23**, 485 (1998).
16. V. Backman, R. Gurjar, K. Badizadegan, L. Itzkan, R.R. Dasari, I.T. Perelman, M.S. Feld, Polarized light scattering spectroscopy for quantitative measurement of epithelial cellular structures in situ, *IEEE Journal of Selected Topics in Quantum Electronics*, **5**, 1019 (1999).

17. R.R. Anderson, Q-switched ruby-laser irradiation of normal human skin - histologic and ultrastructural findings, *Arch Dermatol.* **127**, 1000 (1991).
18. J.A. Muccini, N. Kollias, S.E. Phillips, R.R. Anderson, A.J. Sober, M.J. Stiller, L.A. Drake, Polarized-light photography in the evaluation of photodaging, *J. Am. Acad. Dermatol.* **33**, 765 (1995).
19. S.L. Jacques, J.R. Roman, K Lee, Imaging superficial tissues with polarized light, *Laser Surg. Med.* **26**, 119 (2000).
20. S. G. Demos and R.R. Alfano, Optical fingerprinting using polarisation contrast improvement, *Electronics Letters*, **32**, 24, 2254-2255 (1997).
21. S. G. Demos and R.R. Alfano, Optical polarization imaging, *Appl. Opt.*, **36**, 150-155, (1997).
22. M. S. Patterson, S. Anderson-Engels, Brian C. Wilson, and E. K. Osci, Absorption-spectroscopy in tissue-simulating materials - a theoretical and experimental-study of photon paths, *Appl. Opt.*, **34**, 22-30 (1995)

The promise that optical techniques may offer new medical diagnostic tools has stimulated a great deal of research over the past decade. Optical imaging and optical biopsy are two of the research areas where rapid progress has been achieved indicating that photonic technologies can be particularly suitable in a clinical environment. In the field of optical imaging, there are a number of subsurface imaging techniques such as optical coherence tomography [1], linear and nonlinear emission and harmonic generation imaging [2, 3], and confocal microscopy [4] which are currently under development for clinical evaluation. These techniques provide high resolution images of subsurface structures with the drawback that the imaging depth is very small (i.e., 1 millimeter or less). This problem is caused by the fact that the image arises from photons that reached the target without scattering. As the imaging depth increases, the number of photons that reach the specific depth without scattering decreases exponentially. In order to provide larger imaging depths, other techniques need to be explored.

Utilization of the polarization property of light has recently attracted a great deal of interest in the field of optical imaging. Polarization methods have demonstrated ability to distinguish less scattered photons from diffusive ones [5, 6, 7], improve image quality [8, 9, 10, 11, 12], and provide information regarding the type of tissue [13] or scattering medium [14, 15, 16]. Polarized imaging was also used to better image surface features of the skin [17, 18, 19, 20]. The spectral polarization difference imaging technique (SPDI) was recently proposed as an imaging tool that can provide subsurface imaging at larger depth [21]. The drawback of this technique as proposed is that it requires the use of ultrafast lasers and complicated image normalization procedures.

In this paper, imaging depth of the order of 1-cm is demonstrated using spectral and polarization filtering of the backscattered photons under polarized illumination that is derived from a white light source. This method is a modification of the spectral polarization difference imaging technique with the image normalization procedure simplified to avoid the need for time resolved measurements and ultrafast laser illumination. This experimental work demonstrates a method for deep subsurface imaging in tissues using simple and inexpensive instrumentation.

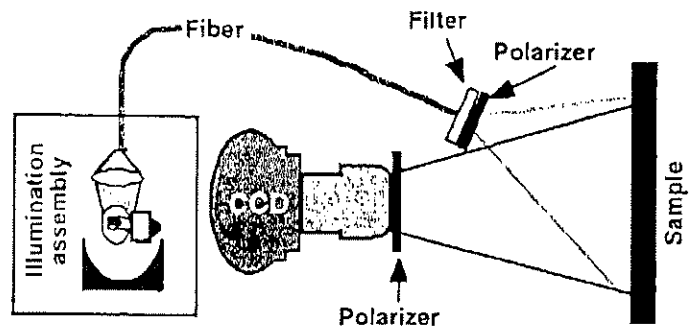


Figure 1. Schematic diagram of the experimental setup.

The experimental setup is shown in fig. 1. A low-power, white-light source coupled to a fiber bundle is used to deliver the illumination light into the sample. A narrow band interference filter is placed at the output of the fiber to achieve illumination of the sample with light of a particular wavelength. To perform this experimental work, a set of four narrow-band-pass filters were used centered at 600-nm, 690-nm, 770-nm and, 970-nm (having FWHM of 9-nm) to record images of the sample at different illumination wavelengths. A polarizer positioned after the optical filter ensured polarized illumination of the sample. Images of the sample in the backscattering geometry were captured using a 50-mm camera lens followed by a liquid nitrogen cooled CCD detector. A second polarizer is positioned in front of the camera lens with its polarization orientation perpendicular to that of the first polarizer in order to record only the perpendicular polarization image component. The imaging plane of the camera lens is located just below the surface of the tissue sample. The depth of focus of the lens was sufficient to allow capture of images of the interesting object located below the surface of the sample without additional adjustment of the focus.

The sample used to demonstrate this subsurface imaging method was a structure prepared using breast chicken tissue as a model medium. A 4-mm diameter, 1-mm thick object composed of a non-absorbing ceramic material was positioned in the middle of the front surface of a  $5 \times 4 \times 1$ -cm<sup>3</sup> (1-cm thick) breast chicken tissue layer and was used as the target to be imaged. The intensity of the backscattered perpendicularly polarized image component of the object is higher (at 850-nm) to that of a 1-cm thick breast chicken tissue by a factor of 0.30 simulating approximately a 3-mm thick fat chicken tissue. Another layer of breast chicken tissue was then positioned so that the object was sandwiched between the two thick breast tissue layers. The sample structure was placed between two glass plates and was slightly compressed to a uniform thickness. The ceramic object was preferred because its size remained unchanged during the experiment allowing for comparison using different imaging depths.

Four perpendicular polarization images of the sample were recorded using the white light illumination assembly described above. The exposure time of the CCD camera to record the image for each illumination wavelength was adjusted so that the digitized image intensity at an arbitrary point at the lower-right part of the image was approximately the same. These digital images were then subtracted (a second image recorded using a shorter illumination wavelength from a first image recorded using a longer illumination wavelength) to obtain a set of SPDI images. Figure 2a shows the perpendicular polarization image of the sample under 600-nm illumination. The presence of the object in this image is not apparent. Figure 2b shows the SPDI image obtained following subtraction of the 770-nm image from the 970-nm image. Similarly, figs. 2c and, 2d show the SPDI images obtained from the subtraction of the 690-nm image from the 770-nm image and, the 600-nm image from the 690-nm image, respectively.

The target object located 1-cm below the surface of the host chicken tissue is viewed with maximum contrast in the image shown in fig. 2b where the 970-nm illumination was used to record the first direct image. This is due to the maximum photon penetration depth which is achieved for the longest in wavelength illumination. The target object is also visible, but with reduced signal to noise ratio, in the image shown in fig. 2c where the 770-nm illumination was used to record the first direct image. Figure 2d indicates that when shorter illumination wavelengths are used to obtain the first direct image, the object is no longer visible because the backscattered photons cannot reach the object and carry its image information.

The improvement of the contrast in the images obtained using the SPDI imaging technique is the result of the removal of a large segment of the image information that is not relevant to the target. In an ordinary imaging arrangement, photons that are backscattered at the surface and just below the surface dominate an image. The information regarding an object located below the surface, which is transported by photons that have reached this depth, is hidden in a strong "background" making its identification difficult. By recording only the cross polarized image component in this imaging method, most of the photons that are back-

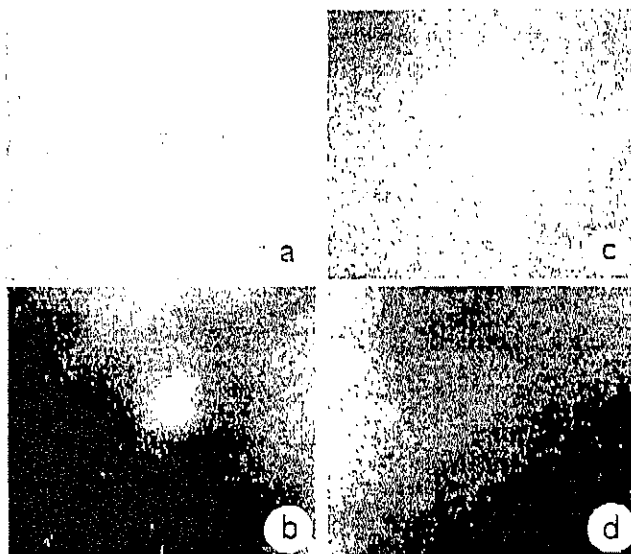
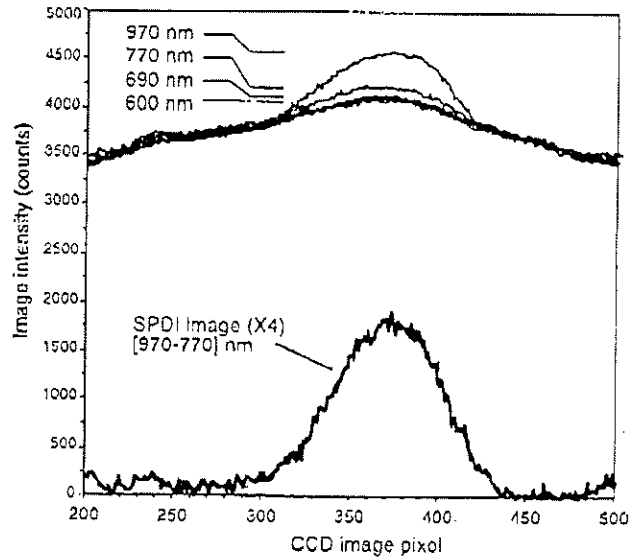


Figure 2: a) Cross polarized image of the tissue sample under 600-nm illumination. SPDI images of the sample obtained using 600-nm, 690-nm, 770-nm and 970-nm illumination reveal the presence of the object located 1-cm underneath the surface: b) [970-770] nm, c) [770-690] nm and, d) [690-600] nm SPDI images.

-scattered at the surface of the host tissue (specular reflection) are rejected [21]. In addition, subtraction of the two images obtained for different illumination wavelengths following normalization cancels out most of the image information arising from photons that were backscattered before reaching the depth where the object of interest is located. This process enhances the relative intensity of the image of an object located below the surface of the host tissue. This is best demonstrated in fig. 3 where the digitized intensity profile across a line that contains the target-object is shown for the four cross-polarized images obtained under 600-nm, 690-nm, 770-nm and, 970-nm that led to the SPDI images shown in figure 2. This figure shows that the information regarding the object is present in the longer illumination wavelength profiles (770-nm and 970-nm) but is rather difficult to be correlated with the object if its presence was not known. This problem is solved by using the SPDI imaging technique which provides a scientifically sound approach to subtract image information that is not relevant to the target object without employing any arbitrarily defined "background subtraction". Figure 3 also shows the digitized intensity profile of the SPDI image demonstrating that the non-relevant to the object "background" arising from light scattering in the homogeneous host tissue is canceled out during image subtraction leading to an image where the target object is viewed with higher contrast.

The experimental results shown in figs. 2, and 3 demonstrate the ability of the technique to acquire deep-subsurface images in tissues. The depth of the target object was chosen for this demonstration (see figs. 2 and 3) so that the object is "visible" (since its presence is known in advance) at longer wavelengths allowing for a demonstration of the basic principles of the technique. Figure 2 shows that the 970-nm photons can reach (and consequently can be used to image) the object located 1-cm underneath the surface of the host breast chicken tissue. Using the 770-nm illumination in the same experiment, the image quality degrades due to the fact that the 770-nm photons barely reach the 1-cm depth before backscattering. Using even shorter wavelengths, the object is no longer visible because it cannot be reached by the imaging photons. In this manner, different depth zones inside the sample can be probed. The maximum imaging depth depends on the scattering and absorption characteristics of the tissue sample at the illumination wavelengths [22]. Using illumination up to 970-nm, the maximum



**Figure 3:** Digitized intensity profile across a line that contains the target-object for the four images obtained under 600 nm, 690 nm, 770 nm and, 970 nm that led to the SPDI images shown in figure 2. The digitized intensity profile of the [970-770] nm SPDI image is also shown for comparison.

imaging depth in this experiment was achieved when the same object was positioned 1.5-cm underneath the surface of the tissue. In this case, imaging was only possible using the 970-nm illumination (SPDI images obtained using 970-nm and 770-nm illumination wavelengths). In general, for imaging depths larger than  $\frac{2}{3}$  of the maximum imaging depth, the target is "visible" only in the SPDI image.

The image processing method used to obtain the SPDI images is realized because the specular reflection image component is removed using polarization means. Without the employment of polarization filtering, there is no normalization procedure that could simultaneously remove both the polarized specular reflection image component and the depo-

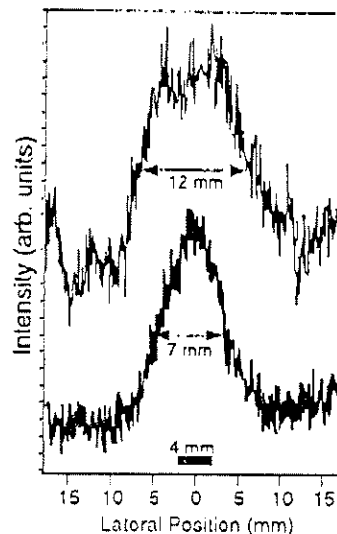


**Figure 4:** The digitized intensity profiles across a line on the SPDI images that contain the 4-mm object when the object is located 7-cm and 1.5-cm below the surface of the host tissue.

-larized image component from the outer tissue layers. The advantage of this technique is that it allows for large imaging depths. This is achieved at the expense of the limited spatial resolution that it can provide. Indeed, the image is formed by photons that have undergone multiple scattering inside the host tissue leading to reduced image resolution when compared to other optical imaging methods [1, 2, 3, 4]. The degradation of the image resolution as a function of the depth at which the target object is located is depicted in fig. 4. The full widths at half maximum of the digitized intensity profiles of the SPDI images of the 4-mm object were measured to be 7-mm and 12-mm when the object is located 1-cm and 1.5-cm below the surface of the host tissue, respectively. The image resolution and/or image quality as a function of the imaging should depend on the scattering and absorption properties of the host medium and the object at the SPDI illumination wavelengths. The results shown in fig. 4 also suggest that the ability of the technique to detect an object may depend on its size and the subsurface depth of its location.

The subsurface spectral polarization difference imaging technique described in this work can be used to highlight differences in absorption or scattering due to the presence of different types of tissue. The utilization of different illuminating wavelengths allows for imaging using photons that reached different penetration depths inside the host tissue. This is what allows for depth profiling. With gradual change of the illuminating wavelengths one can effectively image structures at different depth zones depending on the photon penetration depth of the pair of illumination wavelengths utilized to record the original images. A large (small) difference in the two wavelengths gives rise to a wider (narrower) depth zone. These experimental results indicate that this technique can be used for subsurface imaging at real-time. It also offers the promise of an inexpensive and user-friendly imaging method that can be used in a clinical environment for non-invasive imaging and chemical analysis of tissues in the body.

The research is supported by the Department of Energy. This work was performed at Lawrence Livermore National Laboratory under the auspices of the U.S. Department of Energy under Contract W-7405-Eng-48 through the Institute for Laser Science and Applications and the Materials Research Institute.